

Continuous Hydrogeological Characterisation in Iron Ore Deposits Using Borehole Magnetic Resonance

Kazimierz Trofimczyk

BHP Billiton Limited
Perth, WA
kazek.trofimczyk@bhpbilliton.com

Mark Downey

Downey Data Analysis Pty Ltd
Dudley, NSW
markmerisedowney@gmail.com

Tim Hopper

Qteq Pty L:td
Perth, WA
thopper@qteq.com.au

Tom Neville*

Qteq Pty Ltd
Brisbane, QLD
tneville@qteq.com.au

Benjamin Birt

Kinetic Logging Services
Kewdale, WA
benjamin.birt@kinetic.group

*presenting author asterisked

SUMMARY

In situ dewatering of iron ore deposits is essential for safe and efficient mining operations, as well as reducing requirements for subsequent moisture removal for processing and transportation. Evaluating porosity, residual moisture content, and hydraulic conductivity is key to designing effective dewatering schemes.

Modern borehole magnetic resonance has been used in the oil and gas industry for over twenty years to provide continuous evaluation of porosity, bound and free fluid volumes, and permeability. As such, it is uniquely suited to provide subsurface characterisation data for dewatering scheme design. However, applying these methods in iron ore settings introduces complications that are not observed in typical oil and gas environments due to the high concentrations of paramagnetic and ferromagnetic iron-containing compounds making up the ores. This requires explicitly accounting for the impact of these compounds on surface and diffusional relaxation when estimating fluid volumes and permeability from magnetic resonance measurements.

Development of robust methods for accommodating these effects would allow for practical application of borehole magnetic resonance measurements in iron ore settings, providing continuous and cost effective hydrogeological characterisation.

Key words: iron ore, hydrogeology, magnetic resonance, well logging.

INTRODUCTION

Porosity, residual moisture content, and hydraulic conductivity are key hydrogeological parameters in designing the dewatering schemes that are essential for safe and efficient mining of iron ore deposits. Historically these properties have been determined using a variety of well testing methods, as well as measurements made on core samples. Acquiring core and test data can be both time consuming and costly exercises. Borehole magnetic resonance provides a mean for continuous and cost-effective evaluation of hydrogeological parameters, therefore significant advantages may accrue from utilising these measurements for hydrogeological characterisation.

However, iron ore presents a challenging environment for borehole magnetic resonance logging. Beyond the challenges of simply making a valid and useful borehole magnetic resonance measurement in such environments (Hopper *et al.*, 2017), interpretation of the acquired data presents additional complications. The high concentrations of paramagnetic and ferromagnetic compounds present in iron ore enhance both surface and diffusional relaxation rates. The magnitude of surface relaxivity in such rocks requires that variations in this property be explicitly accounted for. Similarly, the magnitude of internal magnetic field gradients induced by these compounds requires that diffusional relaxation be explicitly accounted for. Both effects are ignored in conventional approaches to borehole magnetic resonance interpretation.

BOREHOLE MAGNETIC RESONANCE

Borehole magnetic resonance (BMR) takes advantage of interactions between hydrogen nuclei and applied (electro)magnetic fields. Hydrogen nuclei possess both angular momentum and a magnetic moment; simplistically they behave like magnets spinning around their magnetic axes. The rate at which the nuclei spin is a function of the magnetic field strength they are exposed to. In a volume of water, or other hydrogen-containing fluids, the magnetic fields of the various hydrogen nuclei in the different fluid molecules will be randomly oriented. If an external magnetic field is introduced, these nuclei will align themselves with the external magnetic field, or polarise. If the effect of this external magnetic field is then removed, the nuclei will over time dephase, until they are again randomly oriented.

A magnetic resonance measurement consists of two steps (Figure 1). In the first step, an external magnetic field B_0 is introduced for a certain period, the wait time or polarisation time. During this period, the hydrogen nuclei align with the B_0 field. In the second step, the effect of the external magnetic field is removed. In practice, this is done by applying an electromagnetic pulse at a frequency in resonance with the spin rate of the hydrogen nuclei, tipping the nuclei through 90° into the secondary B_1 field plane. As well as effectively removing the influence of the B_0 field, this also results in the tipped hydrogen nuclei rotating around the B_0 direction and perpendicular to their magnetic axes, or precessing. The precessing hydrogen nuclei generate an oscillating electromagnetic field that can be detected. This rotation rate is governed by the initial spin rate of the nuclei, which is governed in turn by the B_0 field strength.

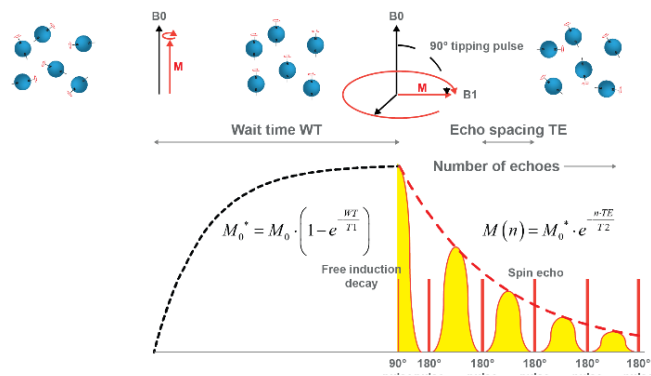


Figure 1: Making a magnetic resonance measurement. Spinning hydrogen nuclei polarise under the influence of an external magnetic field B_0 , and dephase when the influence of this magnetic field is removed; this is achieved by tipping the nuclei through 90° into the B_1 plane using a resonant frequency electromagnetic pulse. While rotating in the B_1 plane, the hydrogen nuclei in turn generate an oscillating electromagnetic signal that is measured. Polarisation and dephasing are quasi-exponential processes characterised by time constants T_1 and T_2 .

When all the hydrogen nuclei are precessing in alignment, a peak electromagnetic signal is generated. However, due to local heterogeneities in the B_0 field, nuclei will precess at different rates and hence quickly dephase, causing a reduction in the net electromagnetic signal. This process, known as free induction decay, is an experimental artefact and is reversible. Applying an appropriate electromagnetic pulse will tip the nuclei by 180° , effectively reversing the direction of rotation. This will bring the faster and slower precessing nuclei back into alignment, causing a new peak signal, or spin echo, to be generated. By applying a series of 180° pulses at a regular interval, or echo spacing, the precessing nuclei can be continually refocussed.

While this is taking place, the hydrogen nuclei are also undergoing irreversible dephasing; this has the effect of moving the axis of rotation of the nuclei out of the B_0 direction so that they no longer contribute to the measured signal. Therefore, over time the amplitude of the spin echoes reduces as nuclei undergo irreversible dephasing. Both polarisation and dephasing of the hydrogen nuclei are quasi-exponential processes, with the rate of polarisation described by the longitudinal relaxation time T_1 and the rate of dephasing described by the transverse relaxation time T_2 . The rates at which polarisation and dephasing take place are controlled by interactions between the magnetic fields of the hydrogen nuclei and other local magnetic fields (Figure 2); this includes interactions with the magnetic fields of other hydrogen nuclei in the fluids, known as bulk relaxation, and interactions with magnetic fields generated by paramagnetic atoms such as iron and manganese that may occur in the minerals bounding fluid-containing pores in a rock, known as surface relaxation. Another contributor to dephasing is diffusional relaxation, which takes place when fluid molecules move to areas of differing magnetic field strength during a magnetic resonance measurement, and are therefore not refocussed successfully by applied 180° pulses. Each of these relaxation mechanisms operates in parallel, and so the overall relaxation rate is dominated by the fastest mechanism.

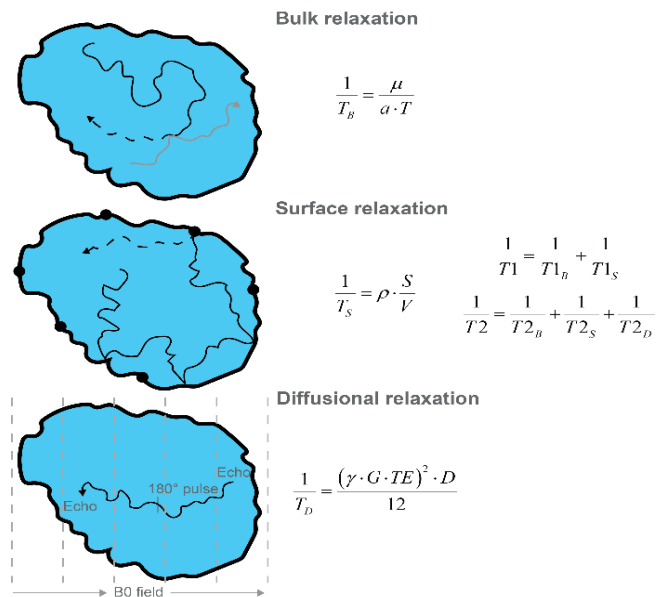


Figure 2: Polarisation (longitudinal relaxation) and dephasing (transverse relaxation) involve two processes, bulk and surface relaxation, occurring in parallel. Dephasing is additionally influenced by diffusional relaxation.

HYDROGEOLOGICAL APPLICATIONS OF BOREHOLE MAGNETIC RESONANCE

For the case of water in a porous medium such as a rock, surface relaxation is the primary mechanism driving polarisation and dephasing of hydrogen nuclei. Surface relaxation involves interactions between the magnetic fields of individual hydrogen nuclei and the magnetic fields generated by paramagnetic atoms such as iron and manganese. Such atoms occur as part of the chemical structure of the rock matrix, and so as fluid molecules move around within pores in a rock, the hydrogen atoms in these molecules may interact with such atoms occurring close to the surfaces of the pores. For a pore of a given volume, the higher its surface area the more likely it is that molecules will approach the pore walls and interact, so the surface-to-volume ratio of a pore is a major control on the rate of surface relaxation. There is also a direct correlation between surface-to-volume ratio and pore size, so the rate of surface relaxation reflects pore size in a rock. For a rock with a range of different pore sizes, a range of relaxation rates will be observed. The signal amplitude related to each relaxation rate indicates the pore volume of the associated pores.

The T2 distribution, or distribution of signal amplitudes related with different transverse relaxation rates, is the fundamental output of a borehole magnetic resonance measurement, concisely summarising the results of the measurement (Figure 3). Signal amplitudes are calibrated to a water reference, so the amplitude related with each relaxation rate is a direct measure of the amount of water, or pore volume, associated with that relaxation rate (pore size). The first hydrogeological property that can be determined from the T2 distribution is the total water content or total porosity, this is simply the sum of amplitudes of each element in the distribution. This porosity is derived directly from the magnetic resonance measurement itself and is independent of any lithology effects.

As well as looking at the sum of amplitudes of all the elements in the T2 distribution, it is useful to look at the sum of amplitudes of the elements within a range of T2 values, corresponding to a range of pore sizes. This can be used to determine the water volume that is free to move, the specific yield, and the water volume held in place in the rock by capillary forces, the specific retention. The T2 values used to separate bound and free fluid are well defined for typical lithologies, or can be determined from core measurements.

The pore size information summarised in the T2 distribution can also be used to estimate permeability. Two main approaches have been employed for permeability estimation from magnetic resonance data. The first approach builds on a range of empirical relationships between porosity, permeability, and irreducible water saturation that have developed over the years; the most common equation of this form is the Timur-Coates permeability equation $k_{Timur-Coates} = 10000 \cdot a \cdot \phi^b \cdot \left(\frac{S_y}{S_r}\right)^c$, where $k_{Timur-Coates}$ is the permeability estimated from the Timur-Coates equation, ϕ is the porosity, S_y is the specific yield, S_r is the specific retention, and a , b , and c are constants with typical values of 1, 4, and 2. The second approach is based on Kozeny-Carmen-type models, with average pore size information coming from the logarithmic or geometric average of the T2 distribution; the most common equation of this form is the SDR permeability equation $k_{SDR} = a \cdot \phi^b \cdot T2_{LM}^c$, where k_{SDR} is the permeability estimated from the SDR equation, $T2_{LM}$ is the logarithmic mean value of the T2 distribution, and a , b , and c are constants with typical values of 4, 4, and 2. Dlubac *et al.* (2013) reviews the origins of these equations, and discusses the application of borehole magnetic resonance-based permeability estimates in aquifer characterisation.

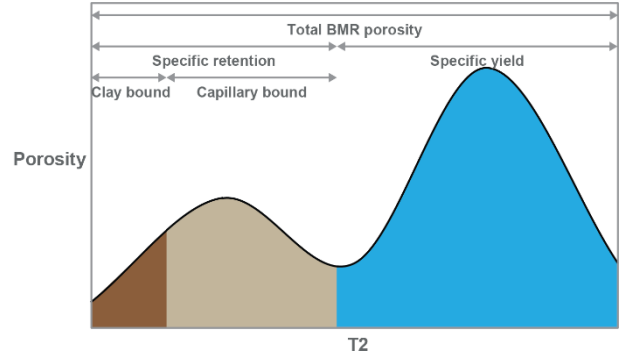


Figure 3: The T2 distribution reflects the volumes of fluid occupying different pore sizes. Integrating amplitudes over the full T2 distribution gives the total porosity, while integrating amplitudes over a range of T2 values allows subdivision into different fluid types based on pore size, such as specific yield and specific retention.

PORE GEOMETRY CONTROLS ON PERMEABILITY

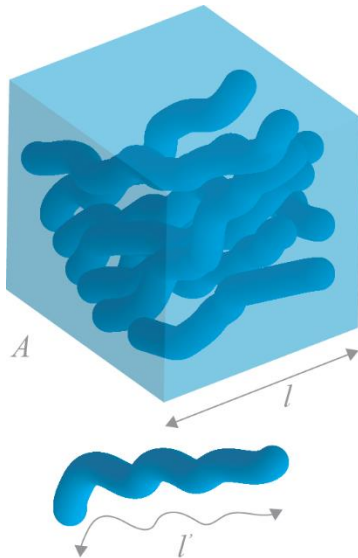


Figure 4: Bundle of capillary tubes model of a porous medium.

Various researchers have investigated the influence of pore geometry on permeability over the past almost one hundred years, with different approaches being taken to describe the key geometrical parameters of a pore system and link them in turn to permeability. One common approach, taken here, is to model the pore system in a rock as a bundle of capillary tubes. Considering the rock representation in Figure 4, Darcy's Law $q = \frac{k}{\mu} \cdot A \cdot \frac{\Delta P}{l}$ can be used to describe the macroscopic flow behaviour of this system, where q is the flow rate, k is the intrinsic permeability, μ is the dynamic viscosity, A is the cross-sectional area, and ΔP is the pressure drop across length l . Similarly, Poiseuille's Law $q = \frac{n \cdot \pi \cdot r^4}{8 \cdot \mu} \cdot \frac{\Delta P}{l'}$ can be used to describe the microscopic flow behaviour of the system, where n is the number of capillaries of radius r and true length l' . As the flow rate is the same from either a macroscopic or microscopic perspective, these two equations can be combined as $k \cdot \frac{A}{l} = \frac{n \cdot \pi \cdot r^4}{8 \cdot l'}$. For this system, the porosity ϕ contained in the capillary tubes is defined by $\phi = \frac{n \cdot \pi \cdot r^2}{A} \cdot \frac{l'}{l}$. Substituting into the previous expression gives $k = \frac{\phi}{8} \cdot \left(\frac{l}{l'}\right)^2 \cdot r^2$ or $k = \frac{\phi}{8 \cdot \tau} \cdot r^2$ where $\tau = \left(\frac{l'}{l}\right)^2$ is the tortuosity. This equation then describes the basic pore geometry controls on permeability: porosity, tortuosity, and pore size.

Although porosity and pore size are reasonably easy to determine, tortuosity is not a property that is easily measured directly. However, similar arguments to those used above to characterise permeability as a function of pore geometry can be used to characterise electrical resistivity. The overall resistivity of a rock containing water-filled capillaries as in Figure 4 is given by $\rho_0 = \frac{\rho_w \cdot A}{n \cdot \pi \cdot r^2} \cdot \frac{l'}{l}$ where ρ_0 is the resistivity of the rock and ρ_w is the resistivity of the water in the capillaries. Substituting for porosity as defined above gives $\rho_0 = \frac{\rho_w}{\phi} \cdot \left(\frac{l'}{l}\right)^2$. Archie (1942) defined the formation factor $F = \frac{\rho_0}{\rho_w}$ and correlated formation factor to porosity by $F = \frac{1}{\phi^m}$ where m is an exponent with a typical value of 2. Using the previous expression for water-filled rock resistivity in Archie's Equation gives $F = \frac{\tau}{\phi} = \frac{1}{\phi^m}$. This can therefore be used as an indirect approach to evaluate

tortuosity. Combining this with the previous expression for permeability gives $k = \frac{1}{8} \cdot \phi^m \cdot r^2$. Similar expressions have been found for permeability, for example in the work of Katz and Thompson (1986).

One remaining challenge with application of such an expression is the appropriate pore size measure to use. In the case of a bundle of capillary tubes model, the appropriate measure is the radius of the capillary tubes. Katz and Thompson employed a critical pore throat radius that could be derived from mercury injection capillary pressure measurements. Johnson and co-workers (Johnson *et al.*, 1986, Herron *et al.*, 1998) introduced a pore geometry parameter Λ that was descriptive of arbitrary pore geometries, and that could be related to the pore surface to pore volume ratio of a rock. In the case of the capillary tube model, pore radius and pore surface to pore volume ratio are related through $\frac{2}{r} = \frac{S}{V}$ where S is the pore surface area and V is the pore volume. Replacing r in the previous permeability expression gives $k = \frac{1}{2} \cdot \phi^m \cdot \left(\frac{V}{S}\right)^2$.

It is this dependence of permeability on porosity and pore surface to pore volume ratio that makes borehole magnetic resonance an attractive approach for estimating permeability, as it can provide direct measurement of both quantities. Although derived empirically, the SDR permeability equation follows directly from the above equation. In water-filled rocks, surface relaxation is typically the dominant relaxation mechanism. The transverse surface relaxation rate $T2_s$ relates directly to pore surface to pore volume ratio through $\frac{1}{T2_s} = \rho \cdot \frac{S}{V}$, where ρ is the surface relaxivity. Substituting into the generalised permeability expression above leads to $k = \frac{1}{2} \cdot \phi^m \cdot (\rho \cdot T2_s)^2$. As surface relaxivity is not a trivial quantity to determine, the pragmatic assumption is taken that it is relatively constant and so can be combined into the constant term in this equation. Furthermore, assuming surface relaxation is the only mechanism contributing to the measured transverse relaxation, and generalising the coefficients in the equation, the SDR permeability equation $k_{SDR} = a \cdot \phi^b \cdot T2_{LM}^c$ results, with $T2_{LM}$ representing the average pore surface to pore volume ratio of the rock.

BOREHOLE MAGNETIC RESONANCE IN IRON ORE DEPOSITS

As described above, two assumptions underlie the estimation of permeability from magnetic resonance measurements: surface relaxation is the dominant or only relaxation mechanism and surface relaxivity can be treated as constant. The first assumption is reasonable in most water-filled rocks. Figure 5 displays the overall transverse relaxation rate resulting from combined bulk and surface relaxation in a water-filled rock. Bulk relaxation only becomes significant in pores sufficiently large that the rate of surface relaxation is comparable to the rate of bulk relaxation, otherwise it can generally be ignored, and the overall transverse relaxation rate can be related directly to pore surface to pore volume ratio.

The second assumption, that surface relaxivity can be considered a constant, is less commonly valid. For sandstones, the average surface relaxivity value (~5 $\mu\text{m}/\text{sec}$) and the typical range of variability in surface relaxivity is such that the relative variations in surface relaxivity are small, and so the assumption that surface relaxivity is constant is reasonable. In carbonates, however, the average surface relaxivity is closer to 1 $\mu\text{m}/\text{sec}$, and so a similar range of variability in surface relaxivity results in a proportionately greater relative variability in surface relaxivity. This variability in surface relaxivity has been recognised as one of the main complications in using magnetic resonance measurements to evaluate flow properties in carbonates, and has led to the explicit inclusion of surface relaxivity in the so-called “carbonate version” of the SDR permeability equation $k_{SDR} = a \cdot \phi^b \cdot (\rho \cdot T2_{LM})^c$ (Allen *et al.*, 2001). A similar argument has been applied to explain the wide variability in transverse relaxation time cut-offs used to differentiate bound and free fluid observed in carbonates. An intrinsic value for pore surface to pore volume ratio may differentiate between bound and free fluid, however this will translate into different transverse relaxation time values as surface relaxivity changes.

Significant variability in surface relaxivity is also expected in iron ores, not because the surface relaxivity is particularly small, but because it is particularly large. The high concentrations of paramagnetic and ferromagnetic compounds present in iron ores and associated deposits are likely to cause significant variations in surface relaxivity, which will influence both the estimation of permeability and the subdivision of total water volume into bound and free fluid fractions. Therefore, analogous to the carbonate approach described above, magnetic resonance interpretation in iron ores must explicitly consider the effect of surface relaxivity.

The presence of large concentrations of paramagnetic and ferromagnetic compounds in iron ores introduces a second complication not observed in most rocks, that of internal gradients. Significant local magnetic field gradients will form when mineral grains of differing magnetic susceptibility are positioned next to each other or next to water-containing pores. These local magnetic field gradients will influence the overall transverse relaxation rate through diffusional relaxation. Diffusional relaxation is a result of molecules moving

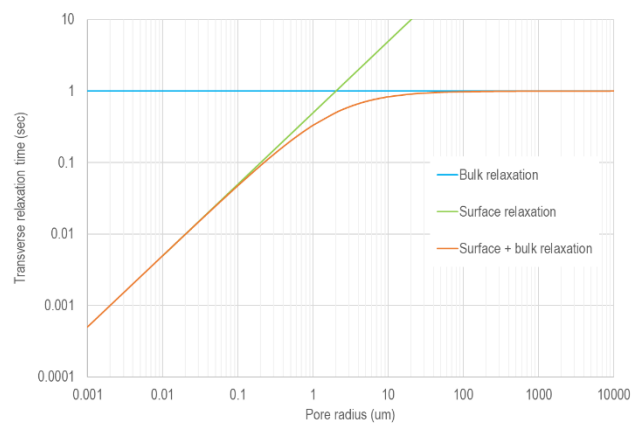


Figure 5: Transverse relaxation rate modelled for cylindrical pores with surface relaxivity of 1 $\mu\text{m}/\text{sec}$ and water bulk relaxation time of 1 second. Bulk relaxation has no significant effect on overall relaxation time unless water is in pores sufficiently large that surface and bulk relaxation times are comparable. Diffusional relaxation is generally ignored in water-filled rocks.

within spatially varying magnetic fields, resulting in individual hydrogen nuclei in these molecules being off resonance with the magnetic field that they are experiencing; this results in an additional apparent relaxation. The diffusional relaxation rate $T2_D$ is described by $\frac{1}{T2_D} = \frac{(\gamma \cdot G \cdot TE)^2 \cdot D}{12}$, where γ is the gyromagnetic ratio of hydrogen, G is the magnetic field gradient, TE is the echo spacing, and D is the fluid diffusion constant. Diffusional relaxation is typically ignored except when high diffusivity fluids such as gases are present, as the overall magnetic field gradient created by a borehole magnetic resonance tool is relatively low. However, where significant local magnetic gradients develop, they can influence the overall transverse relaxation time.

Continuing to ignore bulk relaxation, the overall transverse relaxation time will be defined by both surface and diffusional relaxation $\frac{1}{T2} = \frac{1}{T2_D} + \frac{1}{T2_S} = \frac{1}{T2_D} + \rho \cdot \frac{S}{V}$. This leads to an expression for permeability that captures the influence of paramagnetic and ferromagnetic compounds on both surface and diffusional relaxation as $k = a \cdot \phi^m \cdot \left(\rho \cdot T2 \cdot \frac{T2_D}{T2_D - T2} \right)^2$.

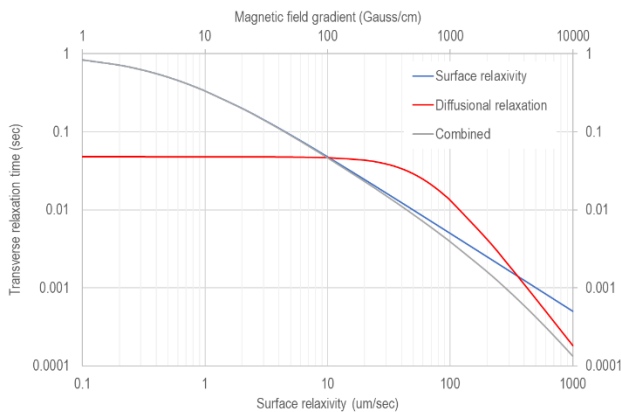


Figure 6: Impact of varying surface relaxivity and internal gradients on the magnitude of surface and diffusional relaxation, and hence transverse relaxation time. Response is for a 0.1 μm cylindrical pore containing water with bulk relaxation time of 1 sec.

diffusional relaxation will increase with higher internal gradients, however as this is an additional multiplicative term that is expected to increase in line with the surface relaxivity, a practical approach is to employ an effective surface relaxivity ρ' that combines both effects, resulting in the following expression for permeability from borehole magnetic resonance in iron ore deposits: $k = a \cdot \phi^m \cdot (\rho' \cdot T2)^2$. As surface relaxivity and the magnitude of internal gradients both relate to the presence of paramagnetic and ferromagnetic components, it is expected that this effective surface relaxivity should vary with magnetic susceptibility, providing a means to determine this quantity independently.

As discussed previously, the same approach can be employed for the definition of T2 cut-offs separating bound and free fluid volumes. The effective surface relaxivity can be combined with an intrinsic pore surface to pore volume ratio marking the separation between bound and free fluid volumes to provide a varying T2 cut-off. Using these modified approaches, borehole magnetic resonance data can be used to determine both residual moisture content or specific retention and hydraulic conductivity, in addition to total water content.

CONCLUSIONS

Iron ores present significant challenges in interpreting magnetic resonance data. The high concentrations of paramagnetic and ferromagnetic compounds present in these deposits enhance both surface and diffusional relaxation effects, and common simplifying assumptions in magnetic resonance interpretation, ignoring variations in surface relaxivity and the role of diffusional relaxation, are not valid.

A method has been developed for accommodating these effects using an effective surface relaxivity term that is correlatable to magnetic susceptibility. The validity of this approach depends on the relative magnitudes of the surface and diffusional relaxation effects in iron ores, which is not fully understood now. Laboratory studies are required to quantify the magnitude of surface and diffusional relaxation effects and better understand how these properties relate to quantities such as chemical composition or magnetic susceptibility so that their effects can be predicted and corrected for.

REFERENCES

Allen, D.F., Boyd, A., Massey, J., Fordham, E.J., Amabeoku, M.O., Kenyon, W.E., and Ward, W.B., 2001, The practical application of NMR logging in carbonates: 3 case studies: SPWLA 42nd Annual Logging Symposium, Houston, Texas.

Archie, G.E., 1942, The electrical resistivity log as an aid in determining some reservoir characteristics. Petroleum Transactions of the AIME, 146, 54-62.

Dlubac, K., Knight, R., Song, Y.-Q., Bachman, N., Grau, B., Cannia, J., and Williams, J., 2013, Use of NMR logging to obtain estimates of hydraulic conductivity in the High Plains aquifer, Nebraska, USA: *Water Resources Research*, 49, 1871-1886.

Herron, M.M., Johnson, D.L., and Schwartz, L.M., 1998, A robust permeability estimator for siliciclastics: 1998 SPE Annual Technical Conference and Exhibition, New Orleans, Louisiana.

Hopper, T.A.J., Trofimczyk, K.K., and Birt, B.J., 2017, Development of a slimhole downhole nuclear magnetic resonance tool for iron ore – some applications and limitations: *Iron Ore 2017*, Perth, Western Australia.

Johnson, D.L., Koplik, J., and Schwartz, L.M., 1986, New pore-size parameter characterizing transport in porous media: *Physical Review Letters*, 57, 2564-2567.

Katz, A.J. and Thompson, A.H., 1986, Quantitative prediction of permeability in porous rock: *Physical Review B*, 34, 8179-8181.